

Benchmarking the Non-flow Contributions to the Elliptic Flow Parameter (v_2) in Proton-Proton Collisions

M. I. Abdulhamid^{1,2,*}, A. M. Hamed¹, E. A. Osama¹, M. Rateb¹, N. K. Sadoun¹ and F. H. Sawy¹

¹Department of Physics, The American University in Cairo, New Cairo 11835, Egypt

²Department of Physics, Faculty of Science, Tanta University, Tanta 31527, Egypt

Abstract. This manuscript reports on the elliptic flow parameter, v_2 , in proton-proton (p-p) collisions using PYTHIA8 event generator simulations. The typical Event Plane (EP) method $v_2(EP)$ as the one used for the real data analysis has been adopted to measure the v_2 of particles composed of different quark flavors, and produced at mid-pseudorapidity $|\eta| \leq 1$ at center-of-mass energy $\sqrt{s} = 200$ GeV and $\sqrt{s} = 13$ TeV. The event plane has been constructed using the soft charged particles with transverse momentum ($p_T < 2$ GeV/c) produced in various η ranges. The pseudorapidity gap technique ($\Delta\eta$) between the particle of interest and the soft charged particles contributed to the event plane constructions has been utilized to benchmark the non-flow contributions. The $v_2^{\pi^\pm, \pi^0}$, $v_2^{J/\psi, \Upsilon, K, D, B}$, and the $v_2^{\gamma_{dir}}$ show similar pattern dependence on the transverse momentum for the same $\Delta\eta$, at both $\sqrt{s} = 200$ GeV and $\sqrt{s} = 13$ TeV. At each center-of-mass energy, the measured v_2 shows obvious dependence on the quark flavor contents where $v_2^{\gamma_{dir}} \leq v_2^{J/\psi, \Upsilon, K, D, B} \leq v_2^{\pi^\pm, \pi^0}$ for similar $\Delta\eta$ gap. The measured v_2 shows slightly higher values at smaller \sqrt{s} for particles of similar values of $\Delta\eta$ gaps, particularly at small $\Delta\eta$ gap. The measured v_2 for all particles shows systematic decreases with increasing the $\Delta\eta$ gap as expected from the previous experimental results. Because PYTHIA8 simulations do not incorporate final state interactions, the $v_2(EP)$ values reported here primarily reflect the non-flow contributions and its dependence on the quark contents, pseudorapidity gap as a function on p_T at each center of mass-energy. These contributions should be carefully subtracted from the signal in real data analysis that employs the same event plane determination algorithm.

keywords: v_2 , Quark-Gluon Plasma, Non-flow contributions, Reaction plane

*Corresponding author: muhammad.ibrahim@science.tanta.edu.eg

1. Introduction

The hydrodynamic flow patterns have been studied extensively in the system created by heavy-ion collisions, as they provide information about the dynamical evolution of the formed system and its transport coefficients [1, 2]. The collective hydrodynamic behavior of the created medium has been assessed using many correlations, e.g., a few-particle correlation and the correlations of the emitted particles concerning the reaction plane orientation. These studies have played an important role in constraining the created medium properties and its dynamics [1, 3]. Recent studies have indicated a prospective examination of the collective and elliptic flow effects in small-sized systems such as proton-proton (p-p) collisions [1]. In contrast to the freely streaming particles where there are no final state interactions; the azimuthal distribution of the produced particles in heavy-ion collisions is expected to be sensitive to the initial geometric overlap of the colliding nuclei, resulting in anisotropic azimuthal distributions with respect to the event plane. The conventional approach for quantifying azimuthal elliptic anisotropy involves expressing particle azimuthal distributions through a Fourier series expansion [4, 5]:

$$\frac{dN}{d\phi} = \frac{N}{2\pi} \left[1 + 2 \sum_{n=1}^{\infty} v_n(p_T, y) \cos[n(\phi_{p_T} - \psi_{EP})] \right] \quad (1)$$

where ϕ is the azimuthal angle and N is the total number of produced particles. The $\frac{dN}{d\phi}$ ratio represents the differential yield of particles as a function of the azimuthal angle. ϕ_{p_T} is the azimuthal angle of the produced particle with a certain value of transverse momentum (p_T). ψ_{EP} is the angle of the event plane and $v_n(p_T, y)$ as a function of p_T and rapidity (y) denotes the coefficient of the n^{th} harmonic, which refers to a specific type of flow. The flow is directed when $n = 1$. The 2^{nd} harmonic, $n = 2$, includes the parameter v_2 , which denotes the ‘‘elliptic flow’’ that strongly depends on the pseudorapidity (η) and transverse momentum (p_T) [3]. The elliptic flow v_2 is given by:

$$v_2(p_T, \eta) = \langle e^{2i(\phi_{p_T} - \psi_{EP})} \rangle = \langle \cos[2(\phi_{p_T} - \psi_{EP})] \rangle \quad (2)$$

where the angular brackets $\langle \dots \rangle$ denote the statistical averaging over particles and events. The correlation of flow is given by eq.1, while any additional contribution will be considered as a ‘‘non-flow’’ [3].

The event plane angle (ψ_{EP}) is a critical experimental observable because it allows for the calculation of flow coefficients. It is conventionally determined from the azimuthal distribution of the produced soft charged particles produced in specific pseudorapidity in a given event, and it may differ from the true reaction plane angle due to the finite number of particles, fluctuations, and measurement errors. On the other hand, ψ_{RP} is a theoretical concept that defines the true plane of symmetry in the collision geometry and it cannot be measured directly. Typically, it refers to the azimuthal angle of the plane defined by the beam axis and the impact parameter vector. The reaction plane angle is commonly determined by the initial geometry of the collision and it is important

in understanding the initial spatial anisotropy of the collision, which gives rise to the elliptic flow [6].

One of the findings of heavy-ion collisions is that the produced particles demonstrate azimuthal anisotropy in the transverse plane. This anisotropy is a result of the initial geometric anisotropy of the collision as evident from the overlap region of the two colliding nuclei being almond-shaped according to kinematic models. Due to the fact that the produced particles are not freely streaming, this geometric anisotropy is then reflected in a momentum azimuthal anisotropy distribution, which is expressed mathematically by the Fourier expansion shown in eq.1. The parameter v_2 , which measures elliptic flow, has been widely studied and is often used as a measure of the momentum azimuthal anisotropy concerning the reaction plane (RP). Quantifying v_2 is important in studying the thermalization of the hypothesized Quark-Gluon Plasma (QGP) by quantifying the collective flow as well as obtaining information about the equation of state for the strongly interacting medium formed in the collisions. As evident in eq.2, to calculate v_2 , one needs to determine the azimuthal angle of the event plane (ψ_{EP}), which serves as a proxy for the true reaction plane (ψ_{RP}). The measured values of v_2 serve as a direct indicator for the degree of collectivity in the medium, such as the possible formation of a thermalized QGP constraining its parameters; e.g. viscosity and entropy.

As the true reaction plane angle (ψ_{RP}) is difficult to determine experimentally, the Event Plane (EP) method is widely used as a practical approach to estimate it. The event plane angle (ψ_{EP}) can be calculated using the following formula [5]:

$$\psi_{EP} = \frac{1}{2} \tan^{-1} \left(\frac{\sum_i \sin(2\phi_i)}{\sum_i \cos(2\phi_i)} \right) \quad (3)$$

where ϕ_i is the azimuthal angle of the i^{th} particle, and the sum runs over all soft particles ($p_T < 2$ GeV/c) produced within certain pseudorapidity range; except the particle of interest to eliminate the auto-correlation [7, 8]. A drawback of this method is that energetic jets produced in the collision can bias the event plane angle determination due to the jet fragmentation, and potentially aligning it with the jet direction. This bias introduces a non-flow related anisotropic component to the elliptic flow (v_2), which must be accounted for to accurately isolate the true flow component.

The eccentricity (ε) with the formula mentioned in eq.4 [5, 9–11] is a measure of how much an ellipse deviates from a perfect circle. For heavy-ion collisions, the overlap region of the colliding nuclei is typically modeled as an ellipse, and the eccentricity is related to the geometry of this ellipse. It provides a comprehensive account of the spatial irregularities within the region of the initial reaction.

$$\varepsilon = \frac{\langle Y^2 - X^2 \rangle}{\langle Y^2 + X^2 \rangle}. \quad (4)$$

In the previous equation, X and Y denote the spatial coordinates of the nucleons in the overlap region of the two colliding nuclei. X is the horizontal axis, and Y is the vertical axis in the transverse plane (i.e. perpendicular to the beam direction). The brackets indicate the averaging over all nucleons.

In terms of the Impact Parameter (IP), the ε value fluctuates from one event to another [5]. The value of IP can be calculated by eq.5 and it is used to determine the centrality of the collision. Eccentricity shapes the elliptic flow of the fireball created in heavy-ion collisions in terms of its expansion [12–14]. There is a correlation between v_2 , representing the final state, and ε in the plane perpendicular to the beam axis, signifying the initial state [15];

$$IP = \sqrt{X_{CM}^2 + Y_{CM}^2} \quad (5)$$

where X_{CM}^2 and Y_{CM}^2 represent the magnitudes of IP in the horizontal and vertical directions, respectively, from the center-of-mass of the overlap region in the transverse plane. If $IP = 0$, the collision is central, while it is considered peripheral (i.e. indicating a smaller overlap region between the colliding nuclei) as $IP > 0$.

The first calculation of v_2 for p-p collision at $\sqrt{s} = 7$ TeV is given in [13]. In a study for p-p collisions at 13 TeV [16], it is found that the value of v_2 is directly proportional to the eccentricity and impact parameter. At the same time, it is inversely proportional to the overlapping area (S), where $S = \pi \sqrt{\langle X_{CM}^2 \rangle \langle Y_{CM}^2 \rangle}$. $\langle X_{CM}^2 \rangle$ and $\langle Y_{CM}^2 \rangle$ denote the averages in the horizontal and vertical directions, respectively, and charged particle distribution at central rapidity ($\frac{dN}{dy}$). The ratio v_2/ε as a function of multiplicity per unit rapidity divided by the overlapping area $\frac{dN/dy}{S}$ can be used as a tool for identifying the elliptic flow [16, 17]. Several studies have been performed to examine the elliptic flow of different mesons. For the D meson, the directed (v_1), elliptic (v_2), and triangular (v_3) flows were studied at $\sqrt{S_{NN}} = 5.02$ TeV of Pb-Pb collision in the ALICE experiment [18] where the triangular flow defines $\langle \cos(3(\phi - \psi_3)) \rangle$ and ψ_3 is the minor axis of the triangular participant. In this study, the values of v_2 and v_3 were compared for pions. At the same center-of-mass energy and collided nuclei, the elliptic flow of muons decay from the charmed and bottom hadrons at different centrality ranges 0-10% and 40-60% were contrasted with theoretical calculations, providing more information about the interaction of the previously mentioned particles with hot-dense matter [19], also the p-p collision is examined at $\sqrt{s} = 13$ TeV. The results show that v_2 was not zero for the Pb-Pb central and semi-peripheral collisions. The elliptic flow of charmed mesons from the Pb-Pb collision at $\sqrt{S_{NN}} = 5.02$ TeV and in mid-centrality (i.e. 30-50%) in the ALICE experiment is reported [20]. The v_2 reconstruction of charmed mesons was at mid-rapidity lower than 0.8 and a momentum range of 1-24 GeV/c. Comparing the previous average values of v_2 with their correspondents at $\sqrt{S_{NN}} = 2.76$ TeV, they were found to be not identical [21]. The v_2 of photons at high p_T corresponds

to the anisotropy in quark momentum and is measured directly after the collision [22]. Conversely, at low p_T , it reflects the substantial momentum anisotropy of pions during hadronic release (i.e. later stages). At $p_T \leq 1\text{-}2$ GeV/c supports information about the development of the QGP fireball [23].

The medium-induced radiative energy loss of partons (jet-quenching) has been proposed as the source for the large observed azimuthal anisotropy at high p_T due to the path-length dependence of the parton energy loss [24]. STAR experiment results show that the magnitude of v_2 at high p_T is larger than the predicted values by pure jet-quenching models [25]. The same results presented no connection between the energy loss and the path length at high p_T through a comparison between correlations of γ_{dir} and π^0 with charged particles [26]. Despite the recent results of PHENIX experiment indicating an in-plane predominance of π^0 particles over those produced out-of-plane, such observations may align with the path-length dependence of energy loss, as reported in the literature [27]. However, the reaction plane determination might remain biased toward the direction of the produced jets.

This paper aims to illustrate the impact of event plane calculation bias caused by jet fragmentations and to establish a benchmark for future research, facilitating the quantification of necessary corrections. In pursuit of this goal, p-p collisions at $\sqrt{s} = 200$ GeV and 13 TeV (i.e. corresponding to the Relativistic Heavy Ion Collider (RHIC) and the Large Hadron Collider (LHC) maximum energies) were simulated using (PYTHIA 8.2). The flow coefficient v_2 has been calculated for mid-rapidity $|\eta| \leq 1$ pions (i.e. π^+ , π^- and π^0), mesons containing heavy quarks (J/ψ , Υ , the D and B meson families) and direct photons (γ_{dir}) representing real photons originating directly from the electromagnetic vertex. The EP method is applied to 30 million simulated events at $\sqrt{s} = 200$ GeV as well as $\sqrt{s} = 13$ TeV. The EP was evaluated using charged particles with $p_T < 2$ GeV in various $|\eta|$ bins as follow: $|\eta| < 1$, $1 < |\eta| < 2$, $2 < |\eta| < 3$, $3 < |\eta| < 4$, $4 < |\eta| < 5$ and $|\eta| > 5$. Therefore, this study has three relevant independent variables that affect the value of v_2 . Those variables are \sqrt{s} , quark flavors, and different $|\eta|$ bins, while RHIC data show a large amount of elliptic flow as predicted by the hydrodynamic models at low p_T , the results at high p_T deviate strongly from the hydrodynamic predictions as expected [28].

The assessment of any residual bias in the determination of the reaction plane, potentially resulting in a positive azimuthal elliptic anisotropy (v_2) signal would be facilitated by measuring the v_2 of direct photons. Furthermore, the $v_2^{\gamma_{dir}}$ would give additional information to help disentangle the various scenarios of direct photon production through the expected opposite contributions to the v_2 [29–31], which could help to confirm the observed binary scaling of the direct photon [32]. Since PYTHIA8 does not incorporate final state interactions [33], any v_2 measurement is not due to the collective flow; however, they are solely due to anisotropies introduced because of biases

in the adopted event plane method. Therefore, the v_2 values reported here should be a benchmark to reduce biases from real data calculations and isolate flow components.

2. Analysis Details

PYTHIA8 (version 8.2) [33] was used to simulate the p-p collisions while maintaining its default parameters, without being tuned to any of the studied collision energies, $\sqrt{s} = 200$ GeV and 13 TeV. The events were generated for each \sqrt{s} energy with a kinematic region of pseudorapidity $|\eta| < 20$ and full azimuth $|\phi| < \pi$. The hadronic decay channel in PYTHIA8 was turned off, to detect the resonances without the need to identify them via the invariant mass reconstruction as in the real experiments. The total number of events generation at each center-of-mass energy is 15 million, where all produced particles per event are identified and their kinematics (η , ϕ , and p_T) were recorded. Table 1 shows more details for the parameters implemented to generate events of interest.

Table 1: Summary of Key PYTHIA8 Parameters Used in the Simulation

Parameter Name	Value
Beams:idA	2212 (proton)
Beams:idB	2212 (proton)
Beams:eCM	200 GeV or 13 TeV
Number of Events	15 million
PhaseSpace:pTHatMin	5.0 GeV
HardQCD:all	on
Charmonium:all	on
Bottomonium:all	on
PromptPhoton:all	on
Random:setSeed	on
PartonLevel:ISR	on
PartonLevel:FSR	on
HadronLevel:Decay	off

2.1. Event Selection Criteria

The event selection criteria are crucial for ensuring the quality and relevance of the data analyzed. Table 2 summarizes the event-level selection cuts applied in this analysis. The selection of p_T and η bins is essential for analyzing flow parameters. The following criteria were used to determine the bin ranges:

- **Transverse Momentum (p_T) Bins:** The p_T bins were selected based on the typical range of transverse momenta observed in proton-proton collisions at the given

center-of-mass energies. At lower p_T values, the collective flow effects are more significant, but for higher p_T values, re-binning has been utilized and the bins are wider to maintain statistical significance, reflecting the reduced number of events in this region [34, 35]. Similar to high-energy experimental setups, soft charged particles ($p_T < 2$ GeV/c), except the particle of interest, produced within the full azimuthal coverage ($|\phi| < \pi$) were used to determine the event plane per event.

- Pseudorapidity (η) Bins:** The pseudorapidity bins were chosen to cover the full kinematic range accessible by the detector, enabling a comprehensive study of the pseudorapidity gap dependence of the flow parameters [36, 37]. To explore the effect of the $\Delta\eta$ gap between the particle of interest and the soft particles used for the event plane reconstructions, the $|\eta| < 20$ range was chosen to cover the mid-pseudorapidity to the forward pseudorapidity. Such coverage ranges in pseudorapidity reach the limit of the zero-degree calorimeter in the typical detector acceptance of high-energy physics experiments. In this analysis, we use the absolute pseudorapidity $|\eta|$ which refers to the magnitude of the individual particles. The event plane (ψ_{EP}) is calculated separately according to eq.3 for each pseudorapidity bin using the azimuthal angles of the soft-charged particles within that bin. These ranges are divided into the following bins: $|\eta| < 1$, $1 < |\eta| < 2$, $2 < |\eta| < 3$, $3 < |\eta| < 4$, $4 < |\eta| < 5$, and $5 < |\eta| < 20$. Different pseudorapidity regions were selected for reaction plane determinations to minimize the non-flow contributions as expected when the forward pseudorapidity detectors were used to determine the event plane.

Table 2: Summary for the Event Selection Criteria for PYTHIA8 Simulation

Criterion	Value
η for all particles	$ \eta < 20$
ϕ range	full (i.e. $-\pi$ to π)
p_T for EP soft particles	$p_T < 2.0$ GeV/c
Phase space cutoff	$p_T > 5.0$ GeV/c

2.2. Generated Data and Quality Assurance

In this study, we rely on generated particle kinematics without incorporating detector effects or reconstruction efficiency corrections that are required due to the limited resolutions of the detectors. Figure 1 shows that particles' distribution also differs as a function of the collision energy. The dN/dp_T distribution at RHIC is better described by the power-law function i.e. $1/p_T^n$, where $n = 7$ for RHIC energy with p_T in the range $0 < p_T < 20$, and $n = 5$ at LHC energy, where $0 < p_T < 40$. The particles' distribution falls more rapidly at RHIC than at LHC. Hence, the distributions at LHC exhibit a

higher kinematics reach as expected due to the difference in the available center-of-mass energy at each collider; and accordingly different regions of the probed parton distributions function.

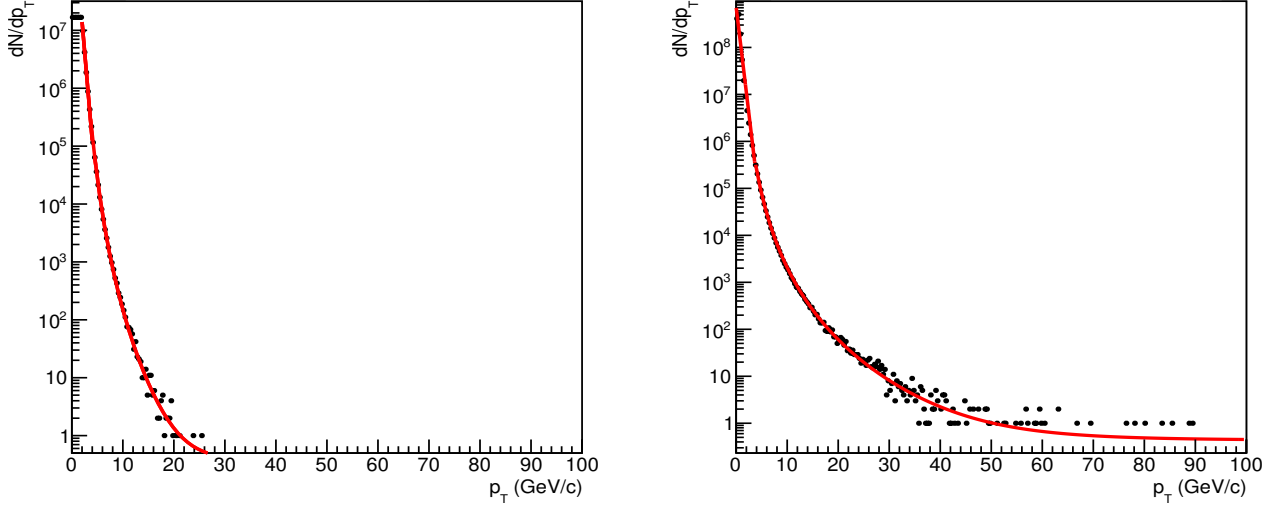


Figure 1: Transverse momentum distribution for $\sqrt{s} = 200$ GeV (left) and $\sqrt{s} = 13$ TeV for p-p collisions (right)

Figure 2 shows the populations of the produced particles in η ($|\eta| \leq 20$) as well as in ϕ ($|\phi| \leq 3.14$ as $\pi \approx 3.14$) for the two different collision energies (i.e. 200 GeV and 13 TeV). Both plots exhibit approximately uniform patterns within the covered kinematic regions of mid-pseudorapidity, more importantly, the distribution indicates the absence of a bias in the azimuthal direction. This is a crucial factor to ensure in the analysis because any bias in the azimuth would affect the calculation of the azimuthal correlation with the reaction plane (v_2).

Figure 3 depicts the distribution of the calculated event plane angle (ψ_{EP}) from eq.3. This uniformity in the distribution indicates an absence of a bias in the event plane. The calculated values of ψ_{EP} are in the range of $-\pi/2 < \psi_{EP} < \pi/2$.

3. Results

The relative azimuthal direction with the event plane angle; v_2 ; of pions: π^0 and π^\pm , heavy mesons: J/ψ , Υ , K^0 , K_0^{*0} , K_0^{*+} , K^+ , D^0 , D^+ , D_0^{*0} , D_0^{*+} , D_s^0 , B^0 , B^+ , B^{*0} , B^{*+} , B_s^0 and B_s^{*0} , and direct photons: γ_{dir} as a function on p_T are presented by figure 4 and 5 at the $\sqrt{s} = 200$ GeV and $\sqrt{s} = 13$ TeV respectively. The pattern of v_2 on p_T , and the effect of center-of-mass energy \sqrt{s} , pseudorapidity gap $|\eta|$ and the quark flavor contents will be addressed in the following context.

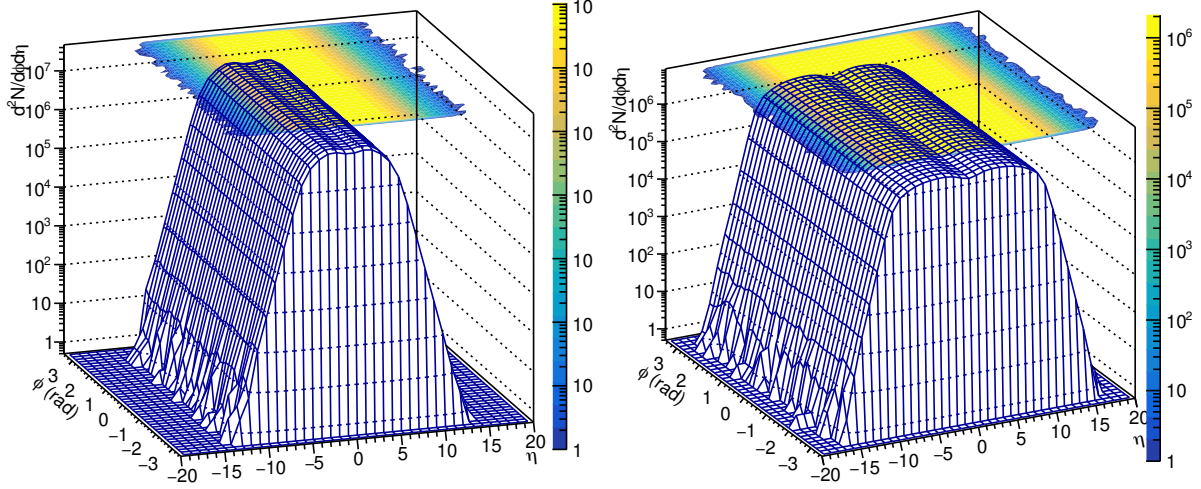


Figure 2: The distribution $d^2N/d\eta d\phi$, at (left) $\sqrt{s} = 200$ GeV and $\sqrt{s} = 13$ TeV (right)

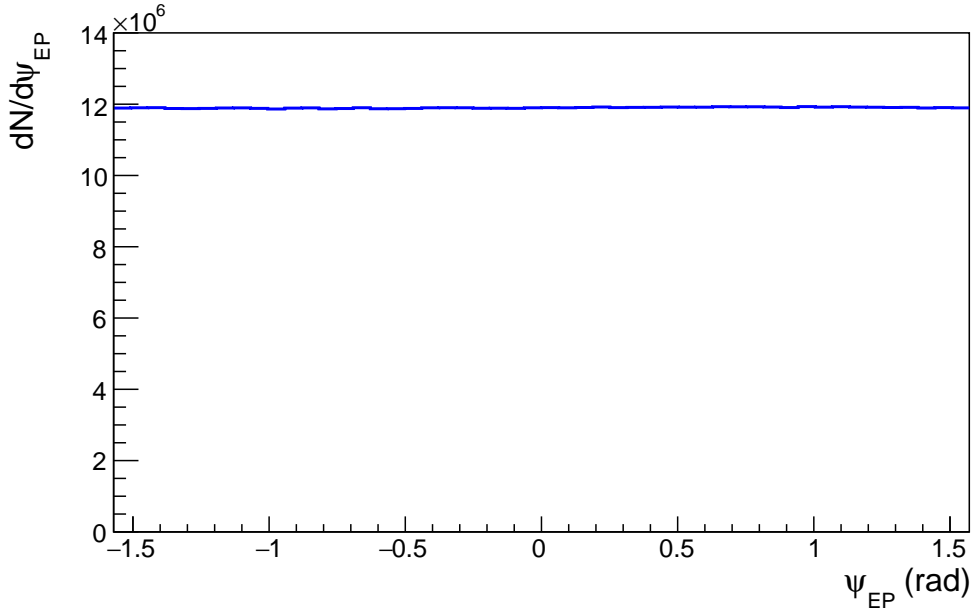


Figure 3: The distribution $dN/d\psi_{EP}$ at $\sqrt{s} = 200$ GeV

3.1. Effect of \sqrt{s} on v_2

A general trend is noticed for the value of v_2 which is getting higher at the lower \sqrt{s} . The effect is more obvious for lower $|\eta|$ bins since the value of v_2 is almost zero for higher $|\eta|$. At lower \sqrt{s} the parton distribution function is dominated by quarks for the same kinematic reach, and hence the quark experiences harder fragmentation than the gluon, therefore, the auto-correlation is expected to be higher. Therefore the v_2 goes reciprocally with the \sqrt{s} at fixed $|\eta|$, for the same quark content at similar p_T .

3.2. Effect of $|\eta|$ on v_2

Generally, the value of v_2 is getting smaller as we go to higher values of the pseudorapidity gap and vanishes at the forward pseudorapidity which indicates the reduction in the non-flow contributions when the forward rapidity regions are used to construct the event plane. The fact that the v_2 of direct photons is finite at the mid-pseudorapidity gap indicates the contribution of the jet fragmentation to the reaction plane determination and hence the non-flow component. The direct photon has no near-side yields and accordingly no azimuthal correlations but it is obvious the away side yields still make a sizable effect and cause non-zero v_2 . The differences in the v_2 values of direct photons at low $|\eta|$ between the two center-of-mass energies can be attributed to the different probed regions in the parton distribution functions as mentioned in the previous section. It is also obvious that the light mesons have higher v_2 compared to the heavy mesons which can be understood in terms of the different fragmentation functions between the light and heavy mesons for the available kinematics reach.

3.3. Effect of quark flavors on v_2

The results show that $v_2^\pi(p_T) > v_2^H(p_T) > v_2^{\gamma^{dir}}(p_T)$, where v_2^π , v_2^H and $v_2^{\gamma^{dir}}$ at low p_T values. On the other hand, there is no obvious trend for higher p_T values due to the insignificant statistics. Regardless of the direct photon v_2 which is used as a reference there is obvious quark flavor dependence. For similar kinematics reach in p_T , and $|\eta|$ at the same \sqrt{s} ; the light mesons show higher v_2 where the bias in the event plane determination is expected to be higher due to the higher multiplicity of the soft particles compared to the case of heavy mesons. Heavy mesons consume more energy to be created than the lighter ones, leaving less energy for the soft particle creations and their multiplicity.

3.4. Effect of p_T on v_2

At both presented \sqrt{s} in this study, the v_2 is finite at low p_T and vanishes at high p_T for all of the particles. Since there are no final state interactions in PYHTIA8, then indeed the observed finite values of v_2 at high p_T are due to the medium effect created in the experiment [25]. At higher p_T less number of produced particles are produced and accordingly the correlations are eliminated. At such high p_T the eccentricity in the spatial coordinates if any is washed out in the momentum space and particles appear to stream freely.

In Fig.4 and Fig.5, the pions, heavy mesons, and direct photons are always selected within $|\eta| \leq 1$, and the $|\eta|$ intervals at the top of each panel represents the pseudorapidity binning for the soft charged particles used for the event plane determination. The higher range of p_T and wider binning choice for pp collisions at $\sqrt{s} = 13$ TeV, compared to $\sqrt{s} = 200$ GeV is for covering the anticipated higher p_T ranges for produced particles.

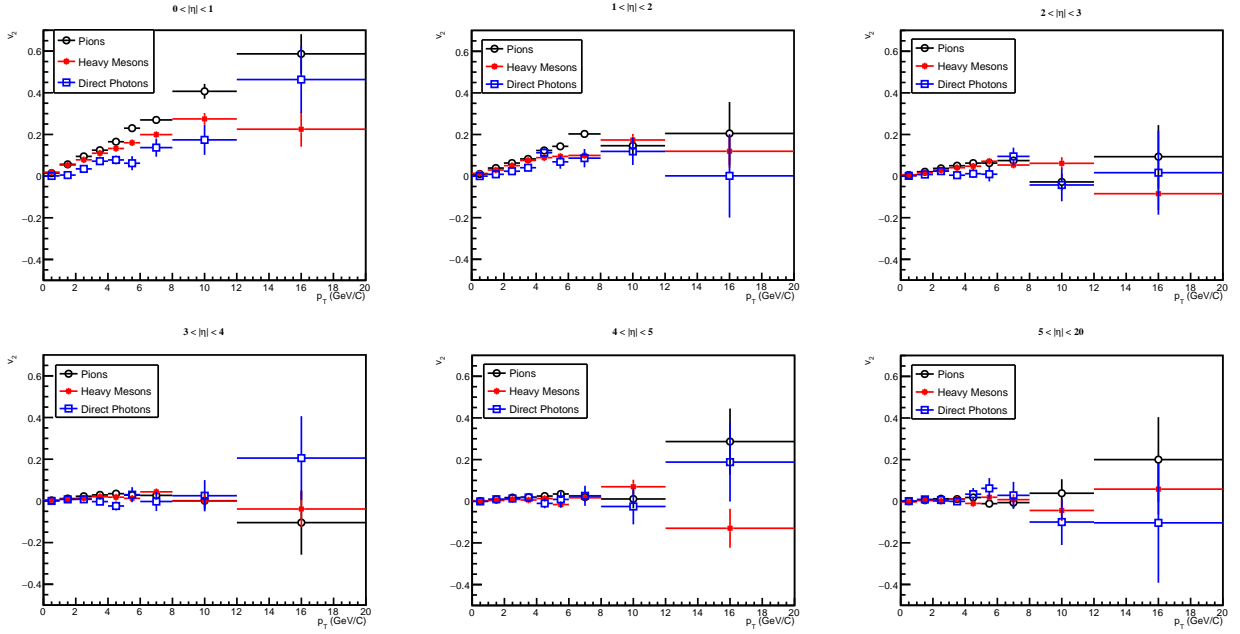


Figure 4: $v_2(p_T)$ for pions, heavy mesons and direct photons at different $|\eta|$ bins for $\sqrt{s} = 200$ GeV with statistical errors

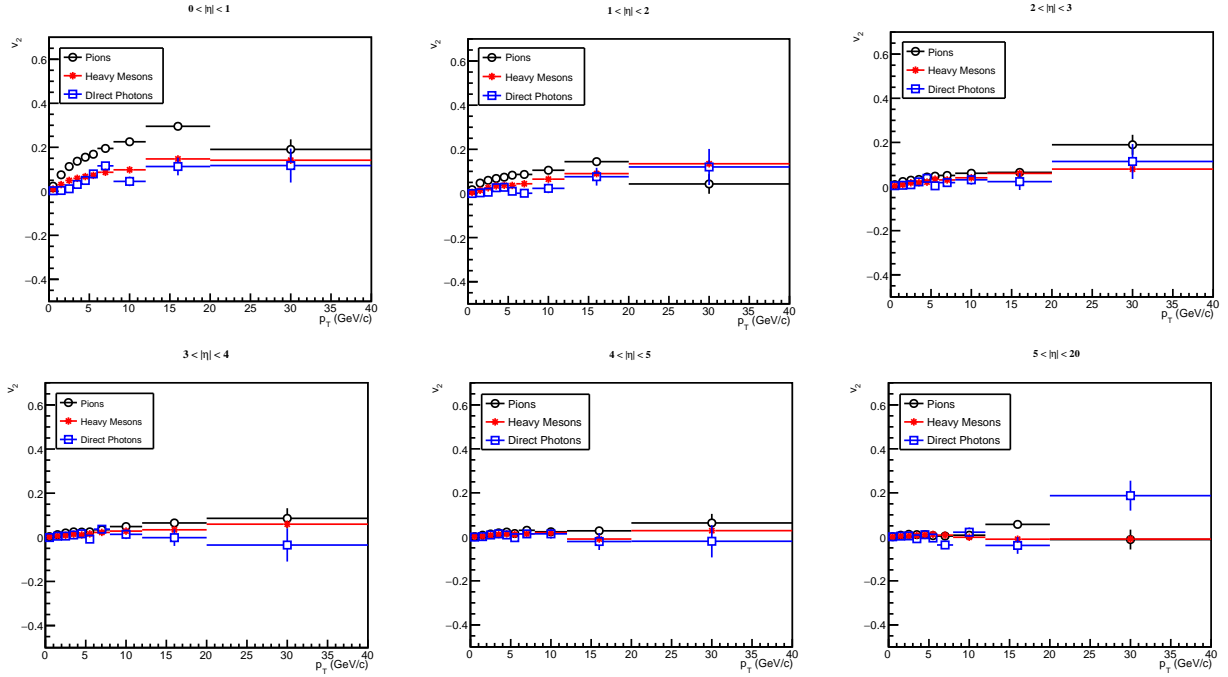


Figure 5: $v_2(p_T)$ for pions, heavy mesons and direct photons at different $|\eta|$ bins for $\sqrt{s} = 13$ TeV with statistical errors

4. Conclusion

In this study, we performed a detailed analysis of the elliptic flow parameter, v_2 , of various particles (light mesons, heavy mesons, direct photons) using the conventional event plane method in proton-proton (p-p) collisions at $\sqrt{s} = 200$ GeV and 13 TeV using PYTHIA8 event generator simulations. The $v_2(p_T)$ for the different particles has shown a similar pattern to that measured in the real experiments. This analysis reports the significant dependence of the elliptic flow parameter on the pseudorapidity gap and its importance in eliminating the non-flow contributions. The interplay between the quark flavor, and the center-of-mass energy has a significant impact on the $v_2(p_T)$ values. Non-flow contributions to the v_2 signal, arising from biases in the event plane determination due to jet fragmentations, are shown in this simulation. Since PYTHIA8 does not include final state interactions, the v_2 values primarily reflect non-flow effects. These contributions should be carefully subtracted in case of experimental data to isolate the true collective flow signal accurately.

5. References

- [1] S. H. Lim, Q. Hu, R. Belmont, K. K. Hill, J. L. Nagle, and D. V. Perepelitsa. Examination of flow and nonflow factorization methods in small collision systems. *Physical Review C*, 100(2):024908, 2019.
- [2] B. Schenke. Flow in heavy-ion collisions—theory perspective. *Journal of Physics G: Nuclear and Particle Physics*, 38(12):124009, 2011.
- [3] M. Luzum. Flow fluctuations and long-range correlations: elliptic flow and beyond. *Journal of Physics G: Nuclear and Particle Physics*, 38(12):124026, 2011.
- [4] S. Voloshin and Y. Zhang. Flow study in relativistic nuclear collisions by fourier expansion of azimuthal particle distributions. *Zeitschrift für Physik C Particles and Fields*, 70:665–671, 1996.
- [5] R. K. Puri, J. Aichelin, S. Gautam, and R. Kumar. *Advances in Nuclear Physics: Structure and Reactions*, volume 257. Springer Nature, 2020.
- [6] S. A. Voloshin, A. M. Poskanzer, and R. Snellings. *Collective Phenomena in Non-Central Nuclear Collisions: Primordial Bulk Plasma Dynamics in Nuclear Collisions at RHIC*. Springer, 2010.
- [7] X. Zhu, M. Bleicher, and H. Stöcker. Elliptic flow analysis in Au+Au collisions at $\sqrt{s_{NN}} = 200$ gev: Fluctuations vs non-flow effects. *Physical Review C*, 72(6):064911, 2005.
- [8] A. M. Poskanzer and S. A. Voloshin. Methods for analyzing anisotropic flow in relativistic nuclear collisions. *Physical Review C*, 58(3):1671, 1998.
- [9] K. Adcox, S. S. Adler, S. Afanasiev, C. Aidala, N. N. Ajitanand, Y. Akiba, A. Al-Jamel, J. Alexander, R. Amirkas, K. Aoki, et al. Formation of dense partonic matter in relativistic nucleus–nucleus collisions at rhic: experimental evaluation by the phenix collaboration. *Nuclear Physics A*, 757(1-2):184–283, 2005.
- [10] R. Snellings. Elliptic flow: a brief review. *New Journal of Physics*, 13(5):055008, 2011.
- [11] M. Luzum and P. Romatschke. Viscous hydrodynamic predictions for nuclear collisions at the lhc. *Physical Review Letters*, 103(26):262302, 2009.
- [12] X.-M. Li, B.-G. Dong, Y.-L. Yan, H.-L. Ma, D.-M. Zhou, and B.-H. Sa. Re-examination for the calculation of elliptic flow and other fourier harmonics. *Modern Physics Letters A*, 25(14):1211–1217, 2010.
- [13] P. Bozek. Elliptic flow in proton–proton collisions at. *Eur. Phys. J. C*, 71:1530, 2011.

- [14] J.-Y. Ollitrault. Anisotropy as a signature of transverse collective flow. *Physical Review D*, 46(1):229, 1992.
- [15] A. Adil, H.-J. Drescher, A. Dumitru, A. Hayashigaki, and Y. Nara. Eccentricity in heavy-ion collisions from color glass condensate initial conditions. *Physical Review C*, 74(4):044905, 2006.
- [16] L. Cunqueiro, J. Dias de Deus, and C. Pajares. Nuclear-like effects in proton–proton collisions at high energy. *The European Physical Journal C*, 65:423–426, 2010.
- [17] I. Bautista, L. Cunqueiro, J. Dias de Deus, and C. Pajares. Particle production azimuthal asymmetries in a clustering of color sources model. *Journal of Physics G: Nuclear and Particle Physics*, 37(1):015103, 2009.
- [18] S. Trogolo. Directed, elliptic and triangular flow of D mesons in ALICE. *PoS*, page 71, 2021.
- [19] Q. Hu. Production and azimuthal anisotropy of muons from heavy flavor decays in small and large systems with atlas. Technical report, ATL-COM-PHYS-2020-403, 2020.
- [20] S. Acharya, D. Adamová, J. Adolfsson, M. M. Aggarwal, G. Aglieri Rinella, M. Agnello, N. Agrawal, Z. Ahammed, N. Ahmad, S. U. Ahn, et al. D-meson azimuthal anisotropy in midcentral pb-pb collisions at $\sqrt{sNN} = 5.02$ TeV. *Physical Review Letters*, 120(10):102301, 2018.
- [21] B. Abelev, J. Adam, D. Adamová, A. M. Adare, M. M. Aggarwal, G. A. Rinella, M. Agnello, A. G. Agocs, A. Agostinelli, Z. Ahammed, et al. D meson elliptic flow in Noncentral pb-pb collisions at $\sqrt{sNN} = 2.76$ TeV. *Physical Review Letters*, 111(10):102301, 2013.
- [22] B. S. Kasmaei and M. Strickland. Photon production and elliptic flow from a momentum-anisotropic quark-gluon plasma. *Physical Review D*, 102(1):014037, 2020.
- [23] R. Chatterjee, E. S. Frodermann, U. Heinz, and D. K. Srivastava. Elliptic flow of thermal photons in relativistic nuclear collisions. *Physical Review Letters*, 96(20):202302, 2006.
- [24] E. V. Shuryak. Azimuthal asymmetry at large p t seem to be too large for a pure “jet quenching”. *Physical Review C*, 66(2):027902, 2002.
- [25] J. Adams, M. M. Aggarwal, Z. Ahammed, J. Amonett, B. D. Anderson, D. Arkhipkin, G. S. Averichev, S. K. Badyal, Y. Bai, J. Balewski, et al. Azimuthal anisotropy and correlations at large transverse momenta in p+p and au+u collisions at $\sqrt{sNN} = 200$ GeV. *Physical Review Letters*, 93(25):252301, 2004.
- [26] B. I. Abelev, M. M. Aggarwal, Z. Ahammed, A. V. Alakhverdyants, B. D. Anderson, D. Arkhipkin, G. S. Averichev, J. Balewski, O. Barannikova, L. S. Barnby, et al. Parton energy loss in heavy-ion collisions via direct-photon and charged-particle azimuthal correlations. *Physical Review C*, 82(3):034909, 2010.
- [27] A. Adare, S. Afanasiev, C. Aidala, N. N. Ajitanand, Y. Akiba, J. Alexander, R. Amirikas, L. Aphecetche, S. H. Aronson, R. Averbeck, et al. Azimuthal anisotropy of π^0 production in Au+Au collisions at $\sqrt{sNN} = 200$ GeV: Path-length dependence of jet quenching and the role of initial geometry. *Physical Review Letters*, 105(14):142301, 2010.
- [28] J. Adams, M. M. Aggarwal, Z. Ahammed, J. Amonett, B. D. Anderson, D. Arkhipkin, G. S. Averichev, S. K. Badyal, Y. Bai, J. Balewski, et al. Experimental and theoretical challenges in the search for the quark–gluon plasma: The star collaboration’s critical assessment of the evidence from rhic collisions. *Nuclear Physics A*, 757(1-2):102–183, 2005.
- [29] B. G. Zakharov. Radiative parton energy loss and jet quenching in high-energy heavy-ion collisions. *Journal of Experimental and Theoretical Physics Letters*, 80(10):617–622, 2004.
- [30] R. J. Fries, B. Müller, and D. K. Srivastava. High-energy photons from passage of jets through quark-gluon plasma. *Physical Review Letters*, 90(13):132301, 2003.
- [31] S. Turbide, C. Gale, and R. J. Fries. Azimuthal asymmetry of direct photons in high energy nuclear collisions. *Physical Review Letters*, 96(3):032303, 2006.
- [32] S. S. Adler, S. Afanasiev, C. Aidala, N. N. Ajitanand, Y. Akiba, J. Alexander, R. Amirikas, L. Aphecetche, S. H. Aronson, R. Averbeck, et al. Centrality dependence of direct photon production in $\sqrt{sNN} = 200$ GeV Au+Au collisions. *Physical Review Letters*, 94(23):232301, 2005.

- [33] T. Sjöstrand, S. Ask, J. R. Christiansen, R. Corke, N. Desai, P. Ilten, S. Mrenna, S. Prestel, C. O. Rasmussen, and P. Z. Skands. An introduction to pythia 8.2. *Computer Physics Communications*, 191:159–177, 2015.
- [34] ALICE Collaboration. Measurement of charm and beauty production at central rapidity versus charged-particle multiplicity in proton-proton collisions at $\sqrt{s} = 7$ TeV. *Journal of High Energy Physics*, 2018(4):108, 2018.
- [35] STAR Collaboration. Experimental and theoretical challenges in the search for the quark-gluon plasma: The star collaboration’s critical assessment of the evidence from rhic collisions. *Nuclear Physics A*, 757(1-2):102–183, 2005.
- [36] J.-Y. Ollitrault. Anisotropy as a signature of transverse collective flow. *Physical Review D*, 48(3):1132, 1993.
- [37] S. A. Voloshin, A. M. Poskanzer, and R. Snellings. Collective phenomena in non-central nuclear collisions. In *Relativistic Heavy Ion Physics*, pages 293–333. Springer, 2008.